JOURNAL OF EDUCATION, SCIENCE AND HEALTH – JESH
Revista de Educação, Ciência e Saúde
DOI: https://www.doi.org/10.52832/jesh.v4i4.448
Home page: https://bio10publicacao.com.br/jesh
e-ISSN: 2763-6119

ACTIVATED CARBON HIGHLY POROUS FROM RECYCLED TOBACCO WASTE: A PROMISING ADSORBENT FOR THIAMETHOXAM REMOVAL

CARVÃO ATIVADO ALTAMENTE POROSO DE RESÍDUOS DE TABACO RECICLADOS: UM ADSORVENTE PROMISSOR PARA REMOÇÃO DE TIAMETOXAM

CARBÓN ACTIVADO ALTAMENTE POROSO DEL RECICLADO DE RESIDUOS DE TABACO: UN ADSORBENTE PROMETEDOR PARA LA ELIMINACIÓN DE TIAMETOXAM

Affonso Celso Gonçalves Jr.[1]*; **Angélica de Fátima Bortolato Piccioli**[2]; **Elio Conradi Jr.**[3]; **Daniel Schwantes**[4]; **Bianca Pierina Carraro**[5]; **Herbert Nacke**[6]; **Emanuel Sobocinski Zanini**[7]

[1]Doutor em Química - Universidade Federal de Santa Catarina (UFSC). Professor na Universidade Estadual do Oeste do Paraná (UNIOESTE) vinculado aos programas de Pós-graduação em Engenharia de Energia na Agricultura (PPGEA) e Pós-graduação em Conservação e Manejo de Recursos Naturais (PPRN), Cascavel (PR), Brasil; [2]Doutora em Química - Universidade Estadual de Maringá (UEM). Pesquisadora de Pós-doutorado no Programa de Pós-graduação em Engenharia de Energia na Agricultura (PPGEA), Universidade Estadual do Oeste do Paraná (UNIOESTE), Cascavel (PR), Brasil; [3]Doutor em Agronomia - Universidade Estadual do Oeste do Paraná (UNIOESTE). Gerente Comercial da Agro Paraná, Açailândia (MA), Brasil; [4]Doutor em Agronomia - Universidade Estadual do Oeste do Paraná (UNIOESTE). Professor na Pontificia Universidad Católica de Chile, Santiago, Chile; [5]Doutora em Engenharia Agrícola - Universidade Estadual do Oeste do Paraná (UNIOESTE). Pesquisadora de Pós-doutorado no Programa de Pós-graduação em Engenharia de Energia na Agricultura (PPGEA), Universidade Estadual do Oeste do Paraná (UNIOESTE), Cascavel (PR), Brasil; [6]Doutor em Agronomia - Universidade Estadual do Oeste do Paraná (UNIOESTE); Diretor de Pesquisa na Forquímica Agrosciência, Cambira (PR), Brasil. [7]Graduado em Química - Instituto Federal do Paraná (IFPR); Mestrando no Programa de Pós-graduação em Conservação e Manejo de Recursos Naturais (PPRN), Universidade Estadual do Oeste do Paraná (UNIOESTE), Cascavel (PR), Brasil.

*Autor correspondente: affonso.celso@unioeste.br

Recebido: 12/07/2024 | **Aprovado**: 10/11/2024 | **Publicado**: 26/11/2024

Resumo: Este trabalho teve como objetivo utilizar resíduos ilícitos de tabaco para produção de carvão ativado (CA) de grande área superficial e sua aplicação na remoção de tiametoxam da água. Por meio da ativação térmica e química, produzimos com sucesso CA derivados de tabaco, incluindo AC800-4-KOH, AC900-4-KOH e AC900-5-KOH. O AC900-4-KOH, em particular, apresentou uma área superficial excepcional de 3.294 $m^2\ g^{-1}$, com grupos funcionais de superfície indicando sua aptidão para adsorção. Em nossa análise abrangente de adsorção, observamos a rápida remoção do tiametoxam, com mais de 95% de adsorção ocorrendo em apenas 5 minutos. O modelo de Freundlich descreve melhor o processo de adsorção, revelando adsorção multicamadas nas superfícies AC inerentemente heterogêneas. Além disso, os resultados da isoterma de Langmuir destacaram a capacidade de adsorção máxima superior do AC900-4-KOH a 150,5 mg g^{-1}, ressaltando seu excepcional potencial de adsorção. As constantes de KLangmuir ilustraram ainda mais a robusta interação tiametoxam-AC, com AC900-5-KOH exibindo a maior afinidade. Nossos resultados demonstram a natureza espontânea, exotérmica e dependente da temperatura da adsorção do tiametoxam ($\Delta G°<0$, $\Delta H°<0$, $\Delta S°>0$), enfatizando sua viabilidade termodinâmica favorável. Além disso, experimentos de eluição com água confirmaram a ausência de liberação significativa de metal dos adsorventes. Este estudo foi pioneiro no uso de resíduos de tabaco reciclado para produzir AC, apresentando capacidades excepcionais de adsorção de tiametoxam. Estas descobertas posicionam o AC como um candidato promissor para aplicações de tratamento de água e remediação ambiental.

Palavras-chave: Neonicotinoides. Biocarvão. Cigarro. Remediação. Superfície funcionalizada.

Abstract: This work aimed to use illicit tobacco residues for the production of activated carbon (AC) with a large

surface area to remove thiamethoxam from water. We successfully produced ACs tobacco-derived through thermal and chemical activation, including AC800-4-KOH, AC900-4-KOH, and AC900-5-KOH. AC900-4-KOH, in particular, displayed an exceptional surface area of 3294 m^2 g^{-1}, with surface functional groups indicating its aptitude for adsorption. In our comprehensive adsorption analysis, we observed rapid thiamethoxam removal, with over 95% adsorption occurring within just 5 minutes. The Freundlich model best described the adsorption process, revealing multilayer adsorption on the inherently heterogeneous AC surfaces. Additionally, Langmuir isotherm results highlighted AC900-4-KOH's superior maximum adsorption capacity at 150.5 mg g^{-1}, underscoring its exceptional adsorption potential. KLangmuir constants further illustrated the robust thiamethoxam-AC interaction, with AC900-5-KOH exhibiting the highest affinity. Our findings demonstrate the spontaneous, exothermic, and temperature-dependent nature of thiamethoxam adsorption ($\Delta G°<0$, $\Delta H°<0$, $\Delta S°>0$), emphasizing its favorable thermodynamic feasibility. Furthermore, water elution experiments confirmed the absence of significant metal release from the adsorbents. This study pioneered the use of recycled tobacco waste to produce AC, showcasing exceptional thiamethoxam adsorption capacities. These findings position the AC as a promising candidate for water treatment and environmental remediation applications.

Keywords: Neonicotinoids. Biochar. Cigarette. Remediation. Functionalized surface.

Resumen: Este trabajo tuvo como objetivo utilizar residuos ilícitos de tabaco para la producción de carbón activado (CA) de gran superficie y su aplicación para eliminar tiametoxam del agua. Mediante activación térmica y química, producimos con éxito carbones activados (CA) derivados del tabaco, incluidos AC800-4-KOH, AC900-4-KOH y AC900-5-KOH. AC900-4-KOH, en particular, mostró una superficie excepcional de 3294 m^2 g^{-1}, con grupos funcionales superficiales que indican su aptitud para la adsorción. En nuestro análisis integral de adsorción, observamos una rápida eliminación del tiametoxam, con más del 95 % de adsorción ocurriendo en solo 5 minutos. El modelo de Freundlich describió mejor el proceso de adsorción, revelando una adsorción multicapa en las superficies de CA inherentemente heterogéneas. Además, los resultados de la isoterma de Langmuir destacaron la capacidad máxima de adsorción superior del AC900-4-KOH a 150,5 mg g^{-1}, lo que subraya su excepcional potencial de adsorción. Las constantes de KLangmuir ilustraron aún más la sólida interacción tiametoxam-AC, donde AC900-5-KOH exhibió la mayor afinidad. Nuestros hallazgos demuestran la naturaleza espontánea, exotérmica y dependiente de la temperatura de la adsorción de tiametoxam ($\Delta G°<0$, $\Delta H°<0$, $\Delta S°>0$), enfatizando su factibilidad termodinámica favorable. Además, los experimentos de elución con agua confirmaron la ausencia de una liberación significativa de metales de los adsorbentes. Este estudio fue pionero en el uso de residuos de tabaco reciclados para producir aire acondicionado y muestra capacidades excepcionales de adsorción de tiametoxam. Estos hallazgos posicionan al AC como un candidato prometedor para aplicaciones de tratamiento de agua y remediación ambiental.

Palabras-clave: Neonicotinoides. Biocarbón. Cigarrillo. Remediación. Superficie funcionalizada.

1 INTRODUCTION

Thiamethoxam is an insecticide widely used in crops in Brazil and worldwide. This neonicotinoid systemic molecule treats seeds of cotton, peanuts, rice, barley, beans, corn, soybeans, and wheat, among others (Brasil, 2021). According to market reports, thiamethoxam is the seventh most-used insecticide in the Brazilian market, with more than 3,400 tons sold yearly (Brasil, 2021).

Due to their high runoff and leaching capacity in surface and groundwater, neonicotinoid pesticides have been frequently detected in aquatic environments, including streams, lakes, and temporary water bodies (González-Pradas *et al.*, 2002). Thiamethoxam has high water solubility (Sw = 4100 mg L^{-1}) and low soil organic carbon partition coefficient (Koc = 68.4) (Brasil, 2022), indicating significant potential for leaching into surface waters. In the scientific literature, it is possible to find several reports of environmental compartments contaminated with thiamethoxam, for example, residues of the insecticide in soil and water in regions that grow rice, citrus, and bananas in the Philippines (Bonmatin *et al.*, 2021), soils in beet crops in Croatia (Gasparic et al., 2020), surface and groundwater around cornfields in the US (Schaafsma et al., 2019) and surface water from the

Danube River, the second longest river in Europe (Iancu *et al.*, 2019).

Adsorption by activated carbons (ACs) is highly viable and effective in removing numerous organic contaminants in various physicochemical conditions, especially for pesticides (Suo *et al.*, 2019; Gonçalves *et al.*, 2022). Activated carbon is produced by controlled pyrolysis without O2, using biomass from different materials such as wood chips, or coconut waste (Badi *et al.*, 2014).

In Brazil, more than 76,080 metric tons of tobacco illegally entered the country in 2019 (Gonçalves *et al.*, 2022), with the seized portion destined for incineration, generating atmospheric pollution with gasses that cause the greenhouse effect and other dangerous contaminants. If considered raw material for producing activated carbon, the tobacco wastes from those cigarettes could have a different destination, promoting an economy closer to circular through the reuse and generation of value to this residue (Hokkanen *et al.*, 2016).

Besides the type of material used in the production of AC, recent publications highlight the improvement in the ability of KOH-modified biomasses to produce adsorbent materials with high surface area on highly micro/mesoporous surfaces and the formation of -OH functional groups on the AC surface (Gonçalves *et al.*, 2023). The effectiveness of KOH activation is relative to other chemical activating agents and can be attributed to the ability of K to quickly form carbon intercalation compounds (Oginni *et al.*, 2019). Furthermore, the K2O formed during the KOH activation process is reduced to K by carbon, resulting in carbon gasification with subsequent CO2 emission leading to the formation of pores (Kamran *et al.*, 2020).

The present study intends to use tobacco waste to produce activated carbon with thermal and chemical activation (KOH as an activating agent) developed by Gonçalvez *et al.* (2023) and test its performance in removing pesticides, through kinetic, equilibrium, and thermodynamic studies of thiamethoxam adsorption.

2 MATERIAL AND METHODS

2.1 Precursor material

The tobacco used in this study was donated by the Federal Revenue Service of Foz do Iguaçu (PR). The experiment was conducted at the Laboratory of Analytical and Environmental Chemistry - (BIOINFRA) and Laboratory of Applied and Environmental Chemistry - (BIOMÉDICAS), Center of Medical and Pharmaceutical Sciences of the Western Paraná State University - Unioeste, *campus* of Cascavel.

2.2 Activated carbon production process and characterization

The production and characterization methodology of the pre-activated carbon Pre-AC-600 and the three activated carbons AC800-4-KOH; AC900-4-KOH and AC900-5-KOH, described in Table 1, used in this article for the adsorption of thiamethoxam followed the procedures described by Gonçalves *et. al.* (2023).

Table 1 - Description of the abbreviations used to name the activated carbons and a short description of their production process

Initials	Nomenclature and short description
Pre-AC600	Pre-activated carbon at 600 ºC (biochar): Treatment of tobacco biomass at 600 ºC in an O_2-free atmosphere in N_2 flow.
AC800-4-KOH	Activated carbon at 800 °C in 4/1 ratio (KOH/CA600): Treatment of tobacco biomass at 600 °C (CA600), followed by a 4:1 KOH:biochar mixture and new pyrolysis at 800 °C in N_2 flow (100 mL min^{-1}).
AC900-4-KOH	Activated carbon at 900 °C in a 4/1 ratio (KOH/CA600): Treatment of tobacco biomass at 600 °C (CA600), followed by a 4:1 KOH:biochar mixture and new pyrolysis at 900 °C in N_2 flow (100 mL min^{-1}).
AC900-5-KOH	Activated carbon at 900°C in a 5/1 ratio (KOH/CA600): Treatment of tobacco biomass at 600 °C (CA600), followed by a 5:1 KOH:biochar mixture and new pyrolysis at 900 °C in N_2 flow (100 mL min^{-1}).

2.3 Chromatographic conditions

Ultra-performance liquid chromatography with diode array detector (UHPLC-DAD, Thermo Scientific UltiMate 3000) was used, equipped with an ACE, C18 column, formed by ultra inert silica, belonging to the octadecyl group, with end-capped technology, 5 μm particles size, 100 Å pore size, 15.5% carbon, pH between 1.5 and 10.0, 25 cm long x 4.6 mm internal diameter.

The chromatographic analysis conditions were: 20 uL of injected sample volume, mobile phase in the proportion 10:90 (v:v) by isocratic mode using HPLC grade acetonitrile (C_2H_3N) and ultrapure water (type I; PERMUTION PURITECH®), run time of 6 min with flow of 1.0 mL min^{-1} and oven and column temperature of 40 ºC. For the UHPLC-DAD analysis, the detector wavelength of 253 nm was used. All data obtained by the analytical experiments performed in the UHPLC-DAD were quantified by the Chromeleon® 7.2 software (THERMO SCIENTIFIC. 2017).

2.4 Artificial contamination of water samples

To evaluate the remediation capacity of ACs in contaminated environments, water samples were artificially contaminated with the insecticide thiamethoxam, prepared from a standard (Thiamethoxam PESTANAL® 250 mg, Sigma-Aldrich; C8H10ClN5O3S Lot #BCBW1778) diluted in ultrapure water (type I).

2.5 Kinetics, equilibrium, and thermodynamics studies of thiamethoxam sorption by tobacco-activated carbon

To determine the ideal time for the adsorption process, as well as to evaluate the adsorption mechanisms in the removal of thiamethoxam, 0.01 g of the ACs and 25 mL of a solution containing 10 mg L^{-1} of thiamethoxam were added to 125 mL Erlenmeyers flasks at pH 5.0. These were shaken at 5, 10, 20, 30, 40, 50, 60, 80, 100 min at 25°C and 200 rpm. Samples were taken at each time interval for later determination of the remaining concentration of thiamethoxam by UHPLC-DAD, following the conditions described in item 2.4.

The results obtained were evaluated using nonlinear mathematical models of the pseudo-first-order of Lagergren

(1898), the pseudo-second-order of Ho & Mckay (1999), and the linear model of intraparticle diffusion of Weber & Morris (1963).

The results obtained in the test above were considered in constructing the adsorption equilibrium isotherms. For that, in 125 mL Erlenmeyers flasks, 0.01 g of ACs were weighed and placed together with 25 mL of thiamethoxam solution pH 5.0 at the following concentrations: 10, 15, 20, 25, 30, and 40 mg L^{-1}. The flasks were then shaken at 200 rpm for 40 min, with subsequent determination of the remaining concentration of thiamethoxam by UHPLC-DAD (as per sub-item 2.4). Such experimental procedures were repeated at 20, 25, 30, 35, and 40 ºC.

The results were evaluated by no linear mathematical models of Langmuir (1917), Freundlich (1907), Sips (1948), Tamer & Berber (2022), Liu (2015), Toth (Steffen et al. 2015), Redlich & Peterson (1959) and Khan (1997).

The constants obtained by fitting Liu (KLiu) at 20, 25, 30, 35, and 40 ºC were used in the Ln(Ke^o) graph versus 1/T. From the interception, the change in entropy was calculated, and by the slope, it was possible to calculate the change in enthalpy (ΔH^o). This procedure allowed the estimation of the thermodynamic parameters Gibbs free energy (ΔG^o), enthalpy (ΔH^o), and entropy (ΔS^o), according to the method proposed by Lima et al. (2019).

Using the OriginPro 8.0 statistical program (ORIGIN 2009), figures and statistical analysis were prepared, as well as parameters that evaluate the fit of the models to the reduced chi-square experimental data (x^2), coefficient of determination (R^2), adjusted coefficient of determination (Adj.R^2) and Pearson's correlation coefficient (r). All nonlinear mathematical models used in kinetics, equilibrium, and thermodynamics studies were obtained using OriginPro 8.0 software, with orthogonal distance regression.

3 RESULTS AND DISCUSSION

3.1 Thiamethoxam adsorption studies

The average removal of thiamethoxam by tobacco ACs over time followed the order AC900-5-KOH (99.15 %) > AC900-4-KOH (99.02 %) > AC800-4-KOH (98.31 %). The ACs evaluated provided thiamethoxam removal rates more excellent than 98% in less than 5 minutes, with chemical equilibrium observed from this point in Table 2.

Table 2 - Nonlinear kinetic parameters of the pseudo-first order (PFO), pseudo-second order (PSO), and linear models of the intraparticle diffusion model in the adsorption of thiamethoxam by AC800-5-KOH, AC900-4-KOH, and AC900-5-KOH.

Kinetic model	AC800-4-KOH	AC900-4-KOH	AC900-5-KOH
PFO			
q_e (calc.) (mg g^{-1})	9.354 ± 0.033	9.550 ± 0.030	9.538 ± 0.039
q_e (calc.) – q_e (exp.)	-0.031 (Δ <1.0%)	0.00 (Δ <1.0%)	-0.001 (Δ <1.0%)
k_1 (min^{-1})	18.436 ± 0.010	19.736 ± 0.010	20.500 ± 0.010
Reduced Chi-Sqr	0.009	0.008	0.010
R-Square (COD)	0.999	0.999	0.999
Adj. R-Square	0.998	0.999	0.999
PSO			
q_e (calc.) (mg g^{-1})	9.433 ± 0.014	9.625 ± 0.012	9.630 ± 0.022
q_e (calc.) – q_e (exp.)	0.048 (Δ <1.0%)	0.075 (Δ <1.0%)	0.091 (Δ <1.0%)
k_2 (g mg^{-1} min^{-1})	0.644 ± 0.084	0.679 ± 0.075	0.677± 0.125
Reduced Chi-Sqr	0.001	0.0007	0.001
R-Square (COD)	0.999	0.999	0.999
Adj. R-Square	0.999	0.999	0.999
%R average	98.30 ± 1.04	99.02 ± 0.96	98.90 ± 1.08
q_e (exp.)	9.385 ± 0.043	9.550 ± 0.093	9.539 ± 0.105
Linear parameters of the intraparticle diffusion model for the segmented line			
AC800-4-KOH			
Parameters	Straight A (5 to 20 min)	Straight B (30 to 50 min)	Straight C (60 to 100 min)
K_{id} (g mg^{-1} $min^{-1/2}$)	0.115 ± 0.037	-0.027 ± 0.009	0.011 ± 0.0002
C_i (mg g^{-1})	8.882 ± 0.126	9.592 ± 0.062	9.275 ± 0.002
Pearson's r	0.952	-0.940	1,000
R-Square (COD)	0.907	0.884	1,000
Adj. R-Square	0.873	0.769	1,000
AC900-4-KOH			
Parameters	Straight A (5 to 20 min)	Straight B (30 to 50 min)	Straight C (60 to 100 min)
K_{id} (g mg^{-1} $min^{-1/2}$)	0.093 ± 0.042	0.045 ± 0.029	-0.015 ± 0.013
C_i (mg g^{-1})	9.156 ± 0.145	9.283 ± 0.183	9.751 ± 0.116
Pearson's r	0.909	0.843	-0.754
R-Square (COD)	0.826	0.710	0.569
Adj. R-Square	0.652	0.421	0.138
AC900-5-KOH			
Parameters	Straight A (5 to 20 min)	Straight B (30 to 50 min)	Straight C (60 to 100 min)
K_{id} (g mg^{-1} $min^{-1/2}$)	0.119 ± 0.033	0.062 ± 0.038	-0.007 ± 0.190
C_i (mg g^{-1})	9.088 ± 0.114	9.171 ± 0.246	9.937 ± 1.702
Pearson's r	0.963	0.850	-0.037
R-Square (COD)	0.927	0.722	0.001
Adj. R-Square	0.855	0.445	-0.997

q_e (calc.) and q_e (exp.): the amount of thiamethoxam retained per gram of adsorbent at equilibrium estimated by the model and calculated experimentally, respectively; k_1: pseudo-first-order constant rate; k_2: pseudo-second order constant rate; k_{id}: intraparticle diffusion constant; Ci: suggests the thickness of the border effect layer; Reduced Chi-Sqr: Reduced Chi-square; R-Square (COD): coefficient of determination R^2; adj. R-Square: adjusted R^2 coefficient of determination. Experimental conditions: 1 g L^{-1} (adsorbent dose); pH 5.0 (solution); 9.668 mg L^{-1} of thiamethoxam concentration; 25°C and stirring at 200 rpm.

Good mathematical fits were observed for PFO and PSO, with a slight discrepancy between q_e (calc.) – q_e (exp.), and excellent values of reduced chi-square (x^2), R^2 [R-Square (COD)], and adjusted R^2 (Adj. R-Square). The rate of adsorption of thiamethoxam, estimated by k_1 (min^{-1}), assumes the following order AC900-5-KOH

(20.500) > AC900-4-KOH (19.736) > AC800-4-KOH (18.436). For the following scenario, k_2 (g mg^{-1} min^{-1}) AC900-4-KOH (0.679) > AC900-5-KOH (0.677) > AC800-4-KOH (0.644) is observed.

Panic *et al.* (2017), when studying the adsorption of thiamethoxam by carbon nanotubes, also obtained good responses to the PFO and PSO models. However, in the literature, several results follow the PSO, as Yang *et al.* (2022) studied the adsorption of thiamethoxam by CA derived from corn stalk residues and found k_2 = 0.032 g mg^{-1} min^{-1}. Fernandes *et al.* (2021) and Freitas *et al.* (2022), when studying AC derived from sugarcane residues, found k_2 values between 0.015 and 0.375 g mg^{-1} min^{-1}, respectively, indicating slower and less intense adsorption compared to our results: 36, 10 and 13 mg g^{-1} at 720, 60 and 10 min, respectively.

Analyzing the standard error values for the nonlinear models of the isotherms at 20 ºC In supplementary material S.1, the Freundlich, Khan, Temkin, and Langmuir models would be the most suitable to describe the experimental data for the three ACs, while Sips, Liu, Toth, and RP overestimate the experimental values.

Regarding Langmuir's q_{max} parameter (mg g^{-1}), the following order is observed: AC900-4-KOH (150.5) > AC900-5-KOH (117.3) > AC800-4-KOH (99.2), suggesting that at 900 °C and with a 4:1 mixing ratio of KOH we have a greater adsorption capacity for thiamethoxam. The $K_{Langmuir}$ values (L mg^{-1}) indicate AC900-5-KOH (2.546) > AC800-4-KOH (1.721) > AC900-4-KOH (1.261), showing that AC900-4-KOH, with higher q_{max}, also shows high interaction between thiamethoxam-AC.

As $R_{Langmuir}$ is very close to zero, the adsorption of thiamethoxam is almost irreversible (Al-ghouti & Da'ana, 2020), and the thiamethoxam-ACs interaction is favorable for the construction of adsorption isotherms (Supplementary material in Figures S2.1, S2.2 and S2.3).

The $K_{Freundlich}$ values [mg g^{-1} (mg $L^{-1})^{-1/n}$] presented in Supplementary material in Table S1, followed the respective order: AC900-5-KOH (87.725) > AC900-4-KOH (82.530) > AC800-4-KOH (56.319), suggesting greater multilayer sorption capacity of thiamethoxam for AC900-5-KOH. The values of $n_{Freundlich}$ are between 2.54 and 1.94 and $1/n_{Freludlich}$ between 0.51 and 0.39 for AC900-5-KOH and AC800-4-KOH, respectively. These results indicate that the adsorption of thiamethoxam by tobacco ACs is favorable ($0 < 1/n < 1$) (Al-Ghouti & Da'ana, 2020).

The values of q_{max} (mg g^{-1}) obtained by the Sips model (Supplementary material in Table S1) show overestimated values, not corresponding adequately to the experimental results. The values of n_{Sips} between 0 and 1, observed in all ACs evaluated, return the premises postulated by Freundlich, suggesting heterogeneity of the surface of the adsorbents and the formation of multilayers (Schwantes *et al.*, 2022). Considering the data mentioned above, the Freundlich model (supplementary material in Table S1 and Figures S2.1, S2.2, and S2.3) is believed to be the most suitable model to describe the adsorption of thiamethoxam for the three materials, suggesting a multilayer adsorption process in an energetically heterogeneous surface of the AC (Milani *et al.*, 2018). Wei *et al.* (2017) also found a multilayer formation of thiamethoxam in AC derived from silkworm droppings. Freitas *et al.* (2022), using AC derived from sugarcane residues, observed the physisorption of thiamethoxam in multilayer.

When comparing the values of q_{max} Langmuir obtained by AC900-4-KOH and AC900-5-KOH with the literature (Table 3), the superiority of these ACs in the removal of thiamethoxam is evident, that is, with values

of q_{max} 167x (Matos *et al.*, 2017), 15x (Fernandes *et al.*, 2021) and 9x (Freitas et al. 2022) smaller than the capacity of AC900-4-KOH.

Table 3 - Comparison between tobacco-based adsorbents and competitors described in the literature regarding removing thiamethoxam from water.

Adsorbent	q_{max} of Langmuir (mg g^{-1})	Reference
AC from Black Acacia Bark	0.9	Matos *et al.* (2017)
Biopolymer-nanoclay compound	1.6	Narayanan *et al.* (2017)
Sugarcane Residue AC	10.2	Fernandes *et al.* (2021)
Sugarcane Residue AC	16.1	Freitas *et al.* (2022)
Hydrogel nanocomposite	17.4	Alammar *et al.* (2020)
AC of activated sludge with $FeCl_3$	81.1	Sanz-Santos *et al.* (2021)
AC-activated sludge with $ZnCl_2$	126.8	Sanz-Santos *et al.* (2021)
AC of corn stalk residue	122.0	Yang *et al.* (2022)
AC800-4-KOH	99.2	This research
AC900-4-KOH	150.5	
AC900-5-KOH	117.3	

Supplementary material in Figures S2.1, S2.2, and S2.3, show a slight reduction in the curvature of the isotherms with the increase in temperature, resulting in a general tendency to reduce the values of the equilibrium constants as a function of the increase in temperature. Furthermore, it is also important to highlight that tobacco-derived ACs show a reduction in the adsorbed amount of thiamethoxam as the initial concentration of this insecticide increases in solution (Supplementary material Figures S2.1, S2.2, and S2.3 in items f). The average values of thiamethoxam removal percentage (Figure 1) obtained were: AC800-4-KOH (95.99%), followed by AC900-4-KOH (98.08%) and AC900-5-KOH (98, 32 %).

The energy and spontaneity during the adsorption processes are further studied by changing the standard free energy (ΔGº), enthalpy (ΔHº), and entropy (ΔSº) (Figure 1 and Table 4). These parameters help us better understand the thiamethoxam adsorption dynamics and physical and chemical nature (Schwantes *et al.*, 2018).

Figure 1 - (a)Average removal of thiamethoxam in the range of 20 to 40 ºC as a function of the use of ACs derived from tobacco modified with KOH (4:1 and 5:1) produced by pyrolysis at 800 and 900 ºC; Linear regression graph 1000 T-1 versus Ln Ke, obtained from the values of KFreundlich in isotherms constructed in the range of 20 to 40 ºC (b).

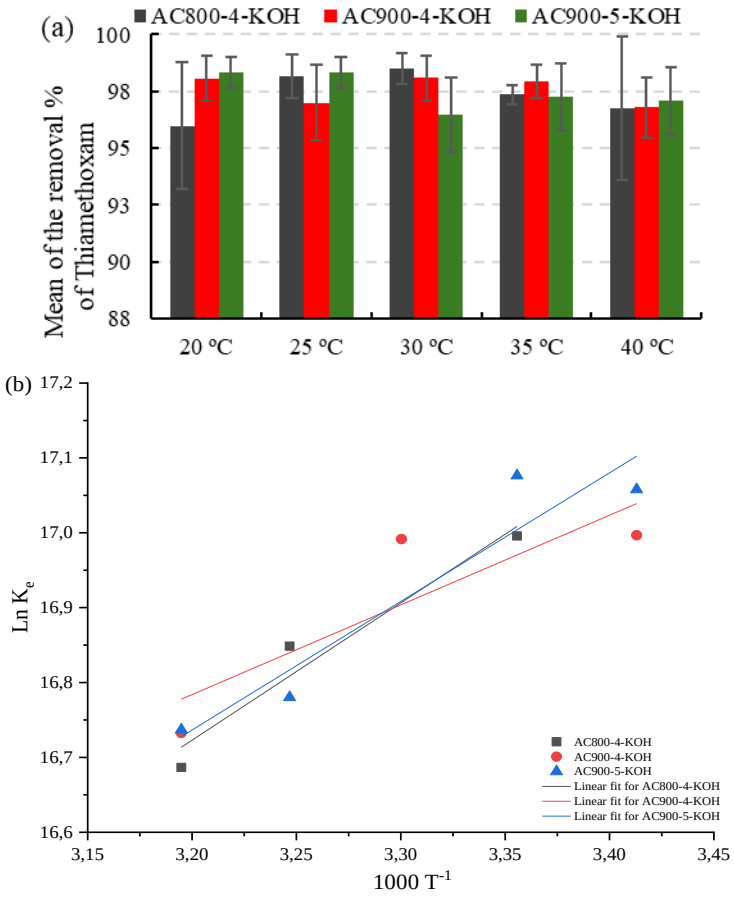

Table 4 – Thermodynamic parameters obtained by Freundlich isotherm in the range of 20 to 40 °C in the adsorption of Thiamethoxam by activated carbons derived from tobacco modified with KOH (4:1 and 5:1) produced by pyrolysis at 800 and 900 °C.

Adsorbent	Temp. (°C)	Thermodynamic parameters						
		Ke (dimensionless)	Δ G° (KJ mol $^{-1}$)	ΔH° (KJ mol $^{-1}$)	ΔS° (J mol $^{-1}$ K $^{-1}$)	Pearson's r	R-Square (COD)	adj. R-Square
AC800-4-KOH	20	16428897.17	-39.78	-15.248	90.241	0.974	0.865	0.954
	25	24050891.49	-41.40					
	30	28731751.83	-42.55					
	35	20760583.55	-42.44					
	40	17656150.31	-42.73					
AC900-4-KOH	20	24075071.34	-40.70	-9.958	107.676	0.948	0.748	0.910
	25	18915453.63	-40.82					
	30	23951704.26	-42.10					
	35	24226775.12	-42.83					
	40	18487407.13	-42.85					
AC900-5-KOH	20	25590388.10	-40.84	-14.277	93.463	0.896	0.496	0.865
	25	26070455.25	-41.60					
	30	17473644.87	-41.32					
	35	19387775.88	-42.27					
	40	18566195.08	-42.86					

K_e: Dimensionless equilibrium constant obtained from the $K_{Freundlich}$ coefficient of isotherms at different temperatures; ΔG°: variation of Gibbs free energy; ΔH°: enthalpy change; ΔS°: entropy change; Pearson's r: Pearson's coefficient; R-Square (COD): coefficient of determination; adj. R-Square: Adjusted coefficient of determination.

Values of ΔG° < 0 (Table 4) reveal that the adsorption of thiamethoxam is spontaneous (Yuan *et al.*, 2020), while values of ΔH° < 0 indicate an exothermic adsorption process. The adsorption capacity gradually

decreases with increasing temperature, indicating a favorable condition for the spontaneous adsorption of thiamethoxam (Wang *et al.*, 2020). Furthermore, $\Delta H^o < 20.9$ suggests physisorption (Roghanizad *et al.*, 2020), while $\Delta S^o > 0$ illustrates increasing randomness in the solid-liquid phase. When ACs capture thiamethoxam molecules, the surface of materials is compressed and disturbed, which leads to an increase in entropy (Yang *et al.* 2022). Therefore, the entropy changes control the force for the adsorption of thiamethoxam by tobacco ACs to occur (Wang *et al.*, 2020).

Yang et al. (2022), using AC derived from corn stalk residues in the adsorption of neonicotinoids, observed an increase in the removal rate accompanied by an increase in temperature, which resulted in non-spontaneous adsorption (ΔG^o = -6.47) and an increase in entropy (ΔS^o = + 178.6) and endothermic process (ΔH^o = + 46.8).

4 CONCLUSIONS

Using tobacco from smuggled cigarettes to produce alternative AC is a real possibility, especially when these are used to remove thiamethoxam from water. Pseudo-first and pseudo-second-order kinetic adsorption models fit the experimental results, with excellent proximity between the q_e (exp.) and q_e (calc.). The adsorption process is rapid, with >98% of thiamethoxam removed in the initial 5 minutes. The following order of rate constant k_1 (min^{-1}) was obtained: AC900-5-KOH (20.500) > AC900-4-KOH (19.736) > AC800-4-KOH (18.436). For k_2 (g mg^{-1} min^{-1}), the following order was observed: AC900-4-KOH (0.679) > AC900-5-KOH (0.677) > AC800-4-KOH (0.644).

In this study, the Freundlich model was more accurate than the other models in describing the adsorption process for the three ACs, due to the high R^2 and variables with low variance, suggesting multilayer adsorption on energetically heterogeneous surfaces.

The maximum adsorption capacity of thiamethoxam estimated by Langmuir followed the order: AC900-4-KOH (150.5 mg g^{-1}) > AC900-5-KOH (117.3 mg g^{-1}) > AC800-4-KOH (99.2 mg g^{-1}). It is essential to highlight that the removal rates obtained were approximately 100%: AC900-5-KOH (99.2%) > AC900-4-KOH (99.0%) > AC800-4-KOH (98.3%). The constant $K_{Langmuir}$ indicated that the materials showed high interaction between thiamethoxam-CA, following the order: AC900-5-KOH (2.546) > AC800-4-KOH (1.721) > AC900-4-KOH (1.261). The thiamethoxam adsorption process was spontaneous ($\Delta G^o < 0$), exothermic, and with a decrease in adsorption capacity with increasing temperature.

Finally, the proposed method for developing ACs from tobacco produced excellent materials extremely efficient in removing thiamethoxam from water. The results demonstrate that tobacco residues can be disposed of not only environmentally correct but also attractive from a technical point of view.

Acknowledgments

This study was financed by the National Council for Scientific and Technological Development (CNPq) and the Coordination of Superior Level Staff Improvement (CAPES). Dr. Affonso Celso Gonçalves Jr. expresses gratitude to CNPq for the productivity grant.

Support

The authors sincerely acknowledge the generous support from the Center for Medical and Pharmaceutical Sciences (CCMF/Unioeste, Brazil) and the Center for Exact and Technological Sciences (CCET/Unioeste, Brazil). In addition, we express our deep appreciation to the Postgraduate Programs in Natural Resources Conservation & Management (PPRN/Unioeste, Brazil) and Energy Engineering in Agriculture (PPGEA/Unioeste, Brazil) for their invaluable contributions to this work.

Lastly, our sincere gratitude extends to the Department of Chemistry at the State University of Londrina (UEL, Brazil) for conducting the characterization evaluations, including FT-IR, SEM, BET, and BJH analyses.

Funding sources

This study has been supported by the National Council for Scientific and Technological Development (CNPq) and the Coordination of Superior Level Staff Improvement (CAPES).

Conflict of interest

The authors declare that there are no conflicts of interest. All authors have approved the final manuscript and agreed with its submission.

Autor's contribution

Affonso Celso Gonçalves Jr.: conceived the monitoring evaluation project, which was fundamental in its idealization and collaboration with the funding agency. He actively validated the methodology definition's result and was crucial to the overall execution of the project. His laboratory provided essential support for most of the analyses, and he contributed significantly to the formal analysis and interpretation of results.

Angélica de Fátima Bortolato Piccioli: Played a crucial role in supervising all chemical analyses and in writing the article.

Élio Conradi Jr.: Modeled and interpreted the collected data and contributed to discussions and interpretation of results.

Daniel Schwantes: Contributed to interpreting results, assisted in conducting laboratory analyses, and writing the article.

Bianca Pierina Carraro: Contributed to the laboratory analysis.

Herbert Nacke: Provided support in carrying out laboratory analyses.

Emanuel Sobocinski Zanini: Provided support in carrying out laboratory analyses.

REFERÊNCIAS

Alammar, A., Park, S.-H., Ibrahim, I., Deepak, A., Holtzl, T., Dumée, L. F., et al. (2020). Architecting neonicotinoid-scavenging nanocomposite hydrogels for environmental remediation. *Applied Materials Today,* 21. https://doi.org/10.1016/j.apmt.2020.100878

Al-Ghouti, M. A., & Da'ana, D. A. (2020). Guidelines for the use and interpretation of adsorption isotherm models: A review. *Journal of Hazardous Materials,* 393. https://doi.org/10.1016/j.jhazmat.2020.122383

Badi, N., Erra, A. R., Robles Hernandez, F. C., Okonkwo, A. O., Hobosyan, M., & Martirosyan, K. S. (2014). Low-cost carbon-silicon nanocomposite anodes for lithium ion batteries. *Nanoscale Research Letters,* 9(1), 1–8. https://doi.org/10.1186/1556-276X-9-360

Bonmatin, J. M., Mitchell, E. A. D., Glauser, G., Lumawig-Heitzman, E., Claveria, F., Bijleveld van Lexmond, M., et al. (2021). Residues of neonicotinoids in soil, water and people's hair: A case study from three agricultural regions of the Philippines. *Science of the Total Environment*, 757. https://doi.org/10.1016/j.scitotenv.2020.143822

BRASIL. Ministério da Agricultura e Pecuária (2021). Coordenação Geral de Agrotóxicos e Afins. Sistema de Agrotóxicos Fitossanitários. Bula Cruiser 350 FS. https://www.gov.br/agricultura/pt-br/assuntos/insumos-agropecuarios/insumos-agricolas/agrotoxicos

BRASIL (2022) Relatórios de comercialização de agrotóxico: boletim 2020. http://ibama.gov.br/phocadownload/qualidadeambiental/relatorios/2020/Vendas_ingredientes_ativos_UF_2020_todos_os_IAs_quimicos.xls

Freitas, D. A., Barbosa, J. A., Labuto, G., Nocelli, R. C. F., & Carrilho, E. N. V. M. (2022). Removal of the pesticide thiamethoxam from sugarcane juice by magnetic nanomodified activated carbon. *Environmental Science and Pollution Research,* 29(53), 79855–79865. https://doi.org/10.1007/s11356-021-18484-1

Fernandes, J. O., Bernardino, C. A. R., Mahler, C. F., Santelli, R. E., Braz, B. F., Borges, R. C., et al. (2021). Biochar Generated from Agro-Industry Sugarcane Residue by Low Temperature Pyrolysis Utilized as an Adsorption Agent for the Removal of Thiamethoxam Pesticide in Wastewater. *Water, Air, and Soil Pollution,* 232(2). https://doi.org/10.1007/s11270-021-05030-5

Freundlich, H. (1907). Ueber Kolloidfällung und Adsorption. *Zeitschrift für Chemie und Industrie der Kolloide*,1(11), 321–331. https://doi.org/10.1007/BF01813604

Gasparic, H. V., Grubelic, M., Uzelac, V. D., Bazok, R., Cacija, M., Drmic, Z., & Lemic, D. (2020). Neonicotinoid residues in sugar beet plants and soil under different agro-climatic conditions. *Agriculture (Switzerland),* 10(10), 1–16. https://doi.org/10.3390/agriculture10100484

González-Pradas, E., Ureña-Amate, M. D., Flores-Céspedes, F., Fernández-Pérez, M., Garratt, J., & Wilkins, R. (2002). Leaching of Imidacloprid and Procymidone in a Greenhouse of Southeast of Spain. *Soil Science Society of America Journal*, 66(6), 1821–1828. https://doi.org/10.2136/sssaj2002.1821

Gonçalves Jr, A. C., Zimmermann, J., Schwantes, D., Tarley, C. R. T., Conradi Junior, E., Henrique Dias de Oliveira, V., et al. (2022). Renewable Eco-Friendly Activated Biochar from Tobacco: Kinetic, Equilibrium and Thermodynamics Studies for Chlorpyrifos Removal. *Separation Science and Technology (Philadelphia),* 57(2), 159–179. https://doi.org/10.1080/01496395.2021.1890776

Gonçalves Jr., A. C., Zimmermann, J., Schwantes, D., Oliveira, V. H. D., Dudczak, F. C., Tarley, C. R. T., Prete, M. C., Snak, A. (2023). Recycling of tobacco wastes in the development of ultra-high surface area activated carbon. *Journal of Analytical and Applied Pyrolysis*, 17, 105965. https://doi.org/10.1016/j.jaap.2023.105965

Ho, Y. S., & Mckay, G. (1999). Pseudo-second order model for sorption processes. *Process Biochemistry,* 34. http://dx.doi.org/10.1016/S0032-9592(98)00112-5

Hokkanen, S., Bhatnagar, A., & Sillanpää, M. (2016). A review on modification methods to cellulose-based adsorbents to improve adsorption capacity. *Water Research,* 91, 156–173. https://doi.org/10.1016/j.watres.2016.01.008

Iancu, V.-I., Petre, J., Galaon, T., & Radu, G. L. (2019). Occurrence of neonicotinoid residues in Danube river and tributaries. *Revista de Chimie,* 70(1), 313–318. https://doi.org/10.37358/rc.19.1.6907

Kamran, U., Choi, J. R., Park, S. J.(2020). A Role of Activators for Efficient CO_2 Affinity on Polyacrylonitrile-Based Porous Carbon Materials. *Frontiers in Chemistry,* 8. https://doi.org/10.3389/fchem.2020.00710

Khan, Y. U., Lawson, D. A., & Tucker, R. J. (1997). Banded radiative heat transfer analysis. *Communications in Numerical Methods in Engineering,* 13(10), 803–813. https://doi.org/10.1002/(SICI)1099-0887(199710)13:10<803::AID-CNM109>3.0.CO;2-D

Lagergren, S. (1898). *About the Theory of So-Called Adsorption of Soluble Substances*. Kungliga Svenska Vetenskapsakademiens Handlingar, 1st ed., 24:1-39.

Langmuir, I. (1917). The constitution and fundamental properties of solids and liquids. Part II.-Liquids. *Journal of the Franklin Institute,* 184(5), 721. https://doi.org/10.1016/s0016-0032(17)90088-2

Lima, E. C., Hosseini-Bandegharaei, A., Moreno-Piraján, J. C., & Anastopoulos, I. (2019). A critical review of the estimation of the thermodynamic parameters on adsorption equilibria. Wrong use of equilibrium constant in the Van't Hoof equation for calculation of thermodynamic parameters of adsorption. *Journal of Molecular Liquids,* 273, 425–434. https://doi.org/10.1016/j.molliq.2018.10.048

Liu, S. (2015). Cooperative adsorption on solid surfaces. *Journal of Colloid and Interface Science,* 450, 224–238. https://doi.org/10.1016/j.jcis.2015.03.013

Manfrin, J., Gonçalves, A. C., Schwantes, D., Conradi, E., Zimmermann, J., & Ziemer, G. L. (2021). Development of biochar and activated carbon from cigarettes wastes and their applications in Pb2+adsorption. *Journal of Environmental Chemical Engineering*, 9(2). https://doi.org/10.1016/j.jece.2020.104980

Manfrin, J., Gonçalves Junior, A. C., Schwantes, D., Zimmermann, J., & Conradi Junior, E. (2021). Effective Cd2+ removal from water using novel micro-mesoporous activated carbons obtained from tobacco: CCD approach, optimization, kinetic, and isotherm studies. *Journal of Environmental Health Science and Engineering,* 19(2),1851–1874. https://doi.org/10.1007/s40201-021-00740-8

Matos, T. T. S., Schultz, J., Khan, M. Y., Zanoelo, E. F., Mangrich, A. S., Araújo, B. R., Navickiene, S., Romão, L. P. C. (2017). Using magnetized (Fe_3O_4/biochar nanocomposites) and activated biochar as adsorbents to remove two neuro-active pesticides from waters. *Journal of the Brazilian Chemical Society,* 28(10), 1975–1987. https://doi.org/10.21577/0103-5053.20170042

Milani, P. A., Consonni, J. L., Labuto, G., & Carrilho, E. N. V. M. (2018). Agricultural solid waste for sorption of metal ions, part II: competitive assessment in multielemental solution and lake water. *Environmental Science and Pollution Research,* 25(36), 35906–35914. https://doi.org/10.1007/s11356-018-1726-7

Narayanan, N., Gupta, S., Gajbhiye, V. T., & Manjaiah, K. M. (2017). Optimization of isotherm models for pesticide sorption on biopolymer-nanoclay composite by error analysis. *Chemosphere,* 173, 502–511. https://doi.org/10.1016/j.chemosphere.2017.01.084

Oginni, O., Singh, K., Oporto, G., Dawson-Andoh, B., McDonald, L., & Sabolsky, E. (2019). Influence of one-step and two-step KOH activation on activated carbon characteristics. *Bioresource Technology Reports,* 7. https://doi.org/10.1016/j.biteb.2019.100266

ORINGIN. (2009). Origin Pro 8 Software. Northampton: OriginLab Corporation.

Panic, S., Guzsvány, V., Kónya, Z., Kukovecz, Á., & Boskovic, G. (2017). Kinetic, equilibrium and thermodynamic studies of thiamethoxam adsorption by multi-walled carbon nanotubes. *International Journal of Environmental Science and Technology,* 14(6), 1297–1306. https://doi.org/10.1007/s13762-016-1237-3

Redlich, O., & Peterson, D. L. (1959). A Useful Adsorption Isotherm. *The Journal of Physical Chemistry,* 63(6), 1024–1024. https://doi.org/10.1021/j150576a611

Roghanizad, A., Karimi Abdolmaleki, M., Ghoreishi, S. M., & Dinari, M. (2020). One-pot synthesis of functionalized mesoporous fibrous silica nanospheres for dye adsorption: Isotherm, kinetic, and thermodynamic studies. *Journal of Molecular Liquids,* 300. https://doi.org/10.1016/j.molliq.2019.112367

Sanz-Santos, E., Álvarez-Torrellas, S., Ceballos, L., Larriba, M., Águeda, V. I., & García, J. (2021). Application of sludge-based activated carbons for the effective adsorption of neonicotinoid pesticides. *Applied Sciences (Switzerland),* 11(7). https://doi.org/10.3390/app11073087

Schaafsma, A. W., Limay-Rios, V., Baute, T. S. & Smith, J. L. (2019). Neonicotinoid insecticide residues in subsurface drainage and open ditch water around maize fields in southwestern Ontario. *PLoS ONE*, 14(4). https://doi.org/10.1371/journal.pone.0214787

Schwantes, D., Gonçalves Jr, A. C., De Varennes, A., & Braccini, A. L. (2018). Modified grape stem as a renewable adsorbent for cadmium removal. *Water Science and Technology,* 78(11), 2308–2320. https://doi.org/10.2166/wst.2018.511

Schwantes, D., Gonçalves Jr., A. C., Perina, H. A., Tarley, C. R. T., Dragunski, D. C., Junior, E. C., & Zimmermann, J. (2022). Ecofriendly Biosorbents Produced from Cassava Solid Wastes: Sustainable Technology for the Removal of Cd^{2+}, Pb^{2+}, and Cr^{total}. *Adsorption Science and Technology, 2022*. https://doi.org/10.1155/2022/5935712

Sips, R. (1948). On the structure of a catalyst surface. *The Journal of Chemical Physics,* 16(5), 490–495. https://doi.org/10.1063/1.1746922

Steffen, V., Cardozo-Filho, L., Silva, E. A., Evangelista, L. R., Guirardello, R., & Mafra, M. R. (2015). Equilibrium modeling of ion adsorption based on Poisson–Boltzmann equation. *Colloids and Surfaces A: Physicochemical and Engineering Aspects,* 468, 159–166. https://doi.org/10.1016/j.colsurfa.2014.11.065

Suo, F., Liu, X., Li, C., Yuan, M., Zhang, B., Wang, J., et al. (2019). Mesoporous activated carbon from starch for superior rapid pesticide removal. *International Journal of Biological Macromolecules,* 121, 806–813. https://doi.org/10.1016/j.ijbiomac.2018.10.132

Tamer, Y., & Berber, H. (2022). Effective removal of crystal violet from aqueous solution by graphene oxide incorporated hydrogel beads as a novel bio-adsorbent: kinetic, isotherm and thermodynamic studies. *Journal of Macromolecular Science, Part A,* 59(4), 315–328. https://doi.org/10.1080/10601325.2022.2033125

THERMO SCIENTIFIC. (2017). Chromeleon 7.2 Chromatography Data Sustem. Waltham: Thermo Fischer Scientific Inc.

Wang, B., Yang, Y., Lu, Y., Wang, W., Wang, Q., Dong, X., & Zhao, J. (2020). Rapid and efficient removal of acetochlor from environmental water using Cr-MIL-101 sorbent modified with 3, 5-Bis(trifluoromethyl)phenyl isocyanate. *Science of the Total Environment,* 710. https://doi.org/10.1016/j.scitotenv.2019.135512

Weber, W. J., & Morris, J. C. (1963). Kinetics of Adsorption on Carbon from Solution. *Journal of the Sanitary Engineering Division,* 89, 31–59. http://dx.doi.org/10.1061/JSEDAI.0000430

Wei, Y., Wu, Y., Chang, Q., Xie, M., Wang, X., Mo, J., et al. (2017). Ultrasonic-assisted modification of a novel silkworm-excrement-based porous carbon with various Lewis acid metal ions for the sustained release of the pesticide thiamethoxam. *RSC Advances,* 7(48), 30020–30031. https://doi.org/10.1039/c7ra04595f

Yang, Y., Ma, X., Yang, C., Wang, Y., Cheng, J., Zhao, J., et al. (2022). Eco-friendly and acid-resistant magnetic porous carbon derived from ZIF-67 and corn stalk waste for effective removal of imidacloprid and thiamethoxam from water. *Chemical Engineering Journal,* 430. https://doi.org/10.1016/j.cej.2021.132999

Yuan, N., Zhang, X., & Wang, L. (2020). The marriage of metal–organic frameworks and silica materials for advanced applications. *Coordination Chemistry Reviews*, 421. https://doi.org/10.1016/j.ccr.2020.213442

ANEXOS E APÊNDICES

Table S1 - Parameters of nonlinear isotherms of Langmuir, Freundlich, Sips, Temkin, Liu, Toth, Redlich-Peterson, and Khan in the adsorption of thiamethoxam by AC800-5-KOH, AC900-4-KOH, and AC900-5-KOH at 20, 25, 30, 35, and 40 ºC.

Parameters	AC800-4-KOH					AC900-4-KOH					AC900-5-KOH				
	20 °C	25 °C	30 °C	35 °C	40 °C	20 °C	25 °C	30 °C	35 °C	40 °C	20 °C	25 °C	30 °C	35 °C	40 °C
Langmuir															
$q_{Langmuir}$ (mg g^{-1})	99.198 ± 8.630	143.198 ± 42.936	142.162 ± 25.179	185.298 ± 49.045	94.906 ± 9.256	150.525 ± 54.707	165.978 ± 74.286	121.11 ± 8.855	147.522 ± 28.436	141.520 ± 4.576	117.248 ± 15.168	138.593 ± 31.739	137.847 ± 21.418	113.010 ± 14.513	110.295 ± 7.954
$K_{Langmuir}$ (L mg^{-1})	1.72104 ± 0.45495	1.44179 ± 0.85324	1.89756 ± 0.69812	0.641 ± 0.26825	2.45668 ± 0.74368	1.2609 ± 0.89031	0.65146 ± 0.52571	2.2485 ± 0.4014	1.33628 ± 0.49701	0.91537 ± 0.06079	2.54594 ± 0.78206	1.66816 ± 0.76412	0.84309 ± 0.27386	1.66348 ± 0.55149	1.642 ± 0.293
$R_{Langmuir}$ (dimensionless)	0.014 to 0.061	0.017 to 0.072	0.013 to 0.055	0.038 to 0.148	0.010 to 0.043	0.019 to 0.081	0.037 to 0.146	0.011 to 0.047	0.018 to 0.077	0.027 to 0.108	0.010 to 0.042	0.015 to 0.062	0.029 to 0.116	0.015 to 0.063	0.015 to 0.063
Reduced Chi-Sqr	38.724	118.468	40.390	30.819	52.124	121.782	145.45	18.409	57.920	2.020	41.782	54.029	43.400	47.501	17.279
R-Square (COD)	0.955	0.862	0.961	0.961	0.930	0.861	0.847	0.981	0.937	0.998	0.950	0.935	0.953	0.948	0.978
Adj. R-Square	0.943	0.828	0.951	0.951	0.912	0.827	0.809	0.976	0.921	0.997	0.937	0.919	0.941	0.935	0.972
Freundlich															
$K_{Freundlich}$ [mg g^{-1} (mg $L^{-1})^{-1/n}$]	56.319 ± 1.756	82.447 ± 5.971	98.494 ± 3.387	71.168 ± 3.030	60.526 ± 2.230	82.530 ± 5.070	64.843 ± 4.379	82.107 ± 2.167	83.050 ± 4.994	63.375 ± 1.401	87.725 ± 4.63	89.371 ± 4.095	59.900 ± 2.043	66.462 ± 1.977	63.646 ± 2.008
$n_{Freundlich}$ (dimensionless)	2.540 ± 0.203	2.066 ± 0.417	1.740 ± 0.133	1.463 ± 0.188	3.217 ± 0.333	1.996 ± 0.380	1.932 ± 0.437	2.058 ± 0.141	1.776 ± 0.271	1.783 ± 0.101	1.938 ± 0.244	1.789 ± 0.196	1.911 ± 0.171	2.015 ± 0.174	2.188 ± 0.194
$1/n_{Freundlich}$ (dimensionless)	0.394	0.484	0.575	0.684	0.311	0.501	0.518	0.486	0.563	0.561	0.516	0.559	0.523	0.496	0.457
Reduced Chi-Sqr	15.153	80.924	14.025	34.212	24.779	62.738	89.753	13.529	62.783	9.522	36.399	24.183	20.404	17.854	19.180
R-Square (COD)	0.982	0.906	0.986	0.956	0.967	0.929	0.906	0.986	0.931	0.990	0.956	0.971	0.978	0.981	0.975
Adj. R-Square	0.978	0.882	0.983	0.945	0.958	0.911	0.882	0.983	0.914	0.988	0.945	0.964	0.972	0.976	0.969
Sips															
q_{Sips} (mg g^{-1})	305.374 ± 544.177	43789.40 1 ± 2.891 10^{7}	25171.92 0 ± 4.562 10^{6}	207.129 ± 274.875	156.219 ± 77.711	96690.33 9 ± 1.453 10^{8}	111384.44 6 ± 2.072 10^{8}	225.075 ± 207.323	176.588 ± 205.795	160.207 ± 24.902	791.766 ± 10535.33 2	32502.93 6 ± 1.036 10^{7}	12841.72 6 ± 1.405 10^{6}	21504.93 0 ± 5.092 10^{6}	147.833 ± 78.349
K_{Sips} (L mg^{-1})	0.048 ± 0.286	2.393 10^{-6} ± 0.003	6.633 10^{-5} ± 0.021	0.517 ± 1.302	0.466 ± 0.919	7.744 10^{-7} ± 0.002	5.767 10^{-7} ± 0.002	0.443 ± 1.112	0.896 ± 2.356	0.692 ± 0.245	0.023 ± 0.711	2.684 10^{-5} ± 0.015	3.717 10^{-5} ± 0.007	9.073 10^{-6} ± 0.004	0.767 ± 1.118
n_{Sips} (dimensionless)	0.483 ± 0.205	0.484 ± 0.467	0.575 ± 0.244	0.950 ± 0.496	0.512 ± 0.167	0.502 ± 0.464	0.518 ± 0.533	0.662 ± 0.233	0.879 ± 0.593	0.910 ± 0.09	0.554 ± 0.568	0.559 ± 0.320	0.525 ± 0.280	0.497 ± 0.307	0.757 ± 0.278

Reduced Chi-Sqr	19.006	107.950	18.748	40.936	21.956	83.707	119.727	15.221	76.241	2.051	48.472	32.289	27.247	23.851	19.099
R-Square (COD)	0.983	0.906	0.986	0.961	0.978	0.928	0.906	0.988	0.937	0.998	0.956	0.971	0.978	0.981	0.982
Adj. R-Square	0.972	0.843	0.977	0.934	0.963	0.881	0.843	0.980	0.896	0.997	0.927	0.952	0.963	0.968	0.969
Temkin															
b_{Temkin} (dimensionless)	0.126 ± 0.012	0.148 ± 0.043	0.094 ± 0.012	0.077 ± 0.011	0.159 ± 0.019	0.166 ± 0.049	0.182 ± 0.059	0.092 ± 0.005	0.083 ± 0.013	0.081 ± 0.004	0.091 ± 0.009	0.106 ± 0.018	0.106 ± 0.019	0.104 ± 0.012	0.100 ± 0.006
A_{Temkin} (L mg^{-1})	22.979 ± 6.531	84.451 ± 85.579	28.806 ± 8.534	9.336 ± 2.478	60.677 ± 27.188	138.953 ± 164.421	128.810 ± 182.433	22.047 ± 3.136	15.769 ± 5.267	9.473 ± 0.985	22.545 ± 5.067	31.421 ± 13.615	15.718 ± 7.164	18.846 ± 5.475	15.509 ± 2.345
Reduced Chi-Sqr	29.904	215.999	62.903	62.595	42.829	226.608	284.517	15.004	89.648	11.004	34.150	89.787	105.446	48.635	12.896
R-Square (COD)	0.965	0.749	0.939	0.920	0.942	0.742	0.701	0.985	0.902	0.989	0.959	0.892	0.886	0.947	0.983
Adj. R-Square	0.956	0.686	0.924	0.900	0.928	0.677	0.627	0.981	0.877	0.986	0.949	0.865	0.858	0.934	0.979
Liu															
q_{Liu} (mg g^{-1})	305.374 ± 544.177	44818.901 ± 3.028 10^{7}	25371.909 ± 4.635 10^{6}	207.129 ± 274.875	156.219 ± 77.711	98743.208 ± 1.515 10^{8}	113744.032 ± 2.161 10^{8}	225.075 ± 207.322	176.588 ± 205.795	160.207 ± 24.902	791.766 ± 10535.335	32772.291 ± 1.054 10^{7}	12934.703 ± 1.426 10^{6}	21649.243 ± 5.161 10^{6}	147.885 ± 78.443
K_{Liu} (L mg^{-1})	0.048 ± 0.286	2.280 10^{-6} ± 0.003	6.541 10^{-5} ± 0.021	0.517 ± 1.302	0.466 ± 0.919	7.425 10^{-7} ± 0.002	5.537 10^{-7} ± 0.002	0.443 ± 1.112	0.896 ± 2.356	0.692 ± 0.245	0.023 ± 0.711	2.644 10^{-5} ± 0.015	3.665 10^{-5} ± 0.00793	8.949 10^{-6} ± 0.004	0.766 ± 1.118
n_{Liu} (dimensionless)	0.483 ± 0.205	0.484 ± 0.467	0.575 ± 0.244	0.950 ± 0.496	0.512 ± 0.167	0.502 ± 0.464	0.518 ± 0.533	0.662 ± 0.233	0.879 ± 0.593	0.910 ± 0.092	0.554 ± 0.568	0.559 ± 0.320	0.525 ± 0.281	0.497 ± 0.307	0.756 ± 0.278
Reduced Chi-Sqr	19.006	107.949	18.747	40.936	21.956	83.706	119.726	15.221	76.241	2.051	48.472	32.288	27.247	23.851	19.099
R-Square (COD)	0.983	0.906	0.986	0.961	0.978	0.928	0.906	0.988	0.937	0.998	0.956	0.971	0.978	0.981	0.982
Adj. R-Square	0.972	0.843	0.977	0.934	0.963	0.881	0.843	0.980	0.896	0.997	0.927	0.952	0.963	0.968	0.969
Toth															
q_{Toth} (mg g^{-1})	1117.49 ± 5826.740	3.083 10^{11} ± 1.460 10^{14}	4.817 10^{6} ± 3.754 10^{8}	83.144 ± 5.530	298.674 ± 464.275	8.586 10^{11} ± 4.296 10^{14}	1.399 10^{10} ± 5.404 10^{12}	381.548 ± 811.133	186.190 ± 377.031	176.465 ± 49.134	1460.090 ± 24374.788	2.878 10^{8} ± 5.183 10^{10}	10^{9} ± 4.55 10^{11}	4.396 10^{9} ± 1.170 10^{12}	186.138 ± 194.248
b_{Toth} (dimensionless)	15.599 ± 74.279	18.009 ± 884.495	0.055 ± 1.556	0.987 ± 0.094	39.403 ± 134.751	1.78128 ± 31.21288	0.168 ± 8.072	2.53913 ± 1.15336	1.259 ± 0.99034	0.864 ± 0.095	2.040 ± 3.930	0.03037 ± 1.63827	0.122 ± 3.149	2.619 ± 21.831	1.938 ± 0.906
n_{Toth} (dimensionless)	0.165 ± 0.288	0.029 ± 0.592	0.074 ± 0.497	44.778 ± 321.148	0.229 ± 0.221	0.02968 ± 0.59776	0.037 ± 0.722	0.3545 ± 0.4109	0.765 ± 1.508	0.772 ± 0.215	0.219± 1.110	0.05267 ± 0.59039	0.042 ± 0.439	0.037 ± 0.524	0.519 ± 0.482
Reduced Chi-Sqr	18.237	110.085	20.087	30.585	24.284	87.792	125.391	14.218	76.909	1.995	47.862	33.703	27.978	24.569	18.005

R-Square (COD)	0.984	0.904	0.985	0.971	0.976	0.925	0.901	0.989	0.937	0.999	0.957	0.970	0.977	0.980	0.983
Adj. R-Square	0.973	0.840	0.976	0.951	0.959	0.875	0.835	0.982	0.895	0.998	0.928	0.949	0.962	0.967	0.971
Redlich-Peterson															
K_{R-P} (L g^{-1})	661.025 ± 917.292	120.106 ± 18.642	5.043 10^{6} ± 9.978 10^{10}	82.240 ± 5.819	1447.852 ± 2046.195	1.736 10^{9} ± 0.010	10^{8} ± 3.282 10^{14}	508.935 ± 422.124	210.801 ± 197.517	146.311 ± 21.346	639.051 ± 1951.734	9.879 10^{6} ± 4.808 10^{11}	4.635 10^{6} ± 1.367 10^{11}	5.146 10^{6} ± 1.608 10^{11}	273.322 ± 182.402
a_{R-P} (L mg^{-1})	10.462 ± 16.335	0.006 ± 736.923	51208.15 2 ± 1.018 10^{9}	0.011 ± 0.112	22.453 ± 33.900	2.104 10^{7} ± 0.010	3.674 10^{6} ± 5.086 10^{12}	5.152 ± 5.185	1.504 ± 2.440	1.192 ± 0.346	6.366 ± 22.313	1.105 10^{5} ± 5.407 10^{9}	77389.18 4 ± 2.294 10^{9}	77428.91 7 ± 2.431 10^{9}	3.129 ± 2.903
β_{R-P} (dimensionless)	0.678 ± 0.110	19.542 ± 4.687 10^{5}	0.425 ± 0.278	10.890 ± 29.963	0.734 ± 0.073	0.499 ± 0.109	0.482 ± 0.290	0.692 ± 0.196	0.923 ± 0.934	0.872 ± 0.120	0.633 ± 0.588	0.44119 ± 0.324	0.476 ± 0.212	0.503 ± 0.286	0.776 ± 0.216
Reduced Chi-Sqr	17.113	159.424	18.700	30.560	28.776	83.650	119.672	13.216	77.139	1.983	47.009	32.244	27.206	23.805	16.781
R-Square (COD)	0.985	0.861	0.986	0.971	0.971	0.929	0.906	0.990	0.937	0.999	0.958	0.971	0.978	0.981	0.984
Adj. R-Square	0.975	0.768	0.977	0.951	0.952	0.881	0.843	0.983	0.894	0.998	0.929	0.952	0.963	0.968	0.973
Khan															
q_{Khan} (mg g^{-1})	21.619 ± 19.054	0.122 ± 2175.542	0.248 ± 327.275	1.163 10^{5} ± 2.332 10^{8}	19.211 ± 16.288	0.079 ± 1688.054	0.056 ± 1500.428	36.161 ± 34.673	155.158 ± 610.301	87.621 ± 39.185	29.655 ± 92.770	0.157 ± 617.137	0.175 ± 728.159	0.296 ± 1075.449	46.864 ± 42.922
b_{Khan} (L mg^{-1})	18.980 ± 31.670	7.051 10^{5} ± 2.594 10^{10}	33311.91 2 ± 7.632 10^{7}	9.506 10^{-4} ± 1.906	59.902 ± 124.894	1.055 10^{6} ± 4.487 10^{10}	814111.79 2 ± 4.152 10^{10}	10.870 ± 15.126	1.262 ± 5.608	1.597 ± 0.852	14.563 ± 65.036	8.455 10^{4} ± 5.923 10^{8}	6.909 10^{4} ± 5.469 10^{8}	54721.32 2 ± 4.006 10^{8}	5.033 ± 6.583
a_{Khan} (dimensionless)	0.655 ± 0.080	0.516 ± 0.164	0.425 ± 0.127	435.843 ± 8.776 10^{5}	0.713 ± 0.059	0.499 ± 0.155	0.482 ± 0.174	0.630 ± 0.150	1.030 ± 2.469	0.776 ± 0.164	0.584 ± 0.426	0.441 ± 0.152	0.476 ± 0.103	0.503 ± 0.159	0.708 ± 0.197
Reduced Chi-Sqr	16.545	107.901	18.703	38.810	30.461	83.652	119.674	12.319	77.223	1.975	46.013	32.246	27.207	23.806	15.861
R-Square (COD)	0.986	0.906	0.986	0.963	0.969	0.928	0.906	0.991	0.937	0.999	0.958	0.971	0.978	0.981	0.985
Adj. R-Square	0.976	0.843	0.977	0.938	0.949	0.881	0.843	0.984	0.894	0.998	0.931	0.952	0.963	0.968	0.974

JOURNAL OF EDUCATION, SCIENCE AND HEALTH – JESH
Revista de Educação, Ciência e Saúde
DOI: https://www.doi.org/10.52832
Home page: https://bio10publicacao.com.br/jesh
e-ISSN: 2763-6119

Figure S 2.1 – Thiamethoxam (TMX) adsorption isotherms for AC800-4-KOH at different temperatures (20, 25, 30, 35, and 40 °C) according to nonlinear models of Langmuir (a), Freundlich (b), Sips (c), Temkin (d), Liu (e), Toth (f), Redlich - Peterson (g) and Khan (h); Variation of Thiamethoxam removal by AC800-4-KOH as a function of different temperatures and initial concentration of insecticide (i). Experimental conditions: 0.01 g of adsorbent, pH 5.0, contact time of 40 min., 200 rpm. Variables: Temperature 20, 25,30,35 and 40 °C, and thiamethoxam concentration: 10, 15, 20, 25, 30 e 40 mg L $^{-1}$.

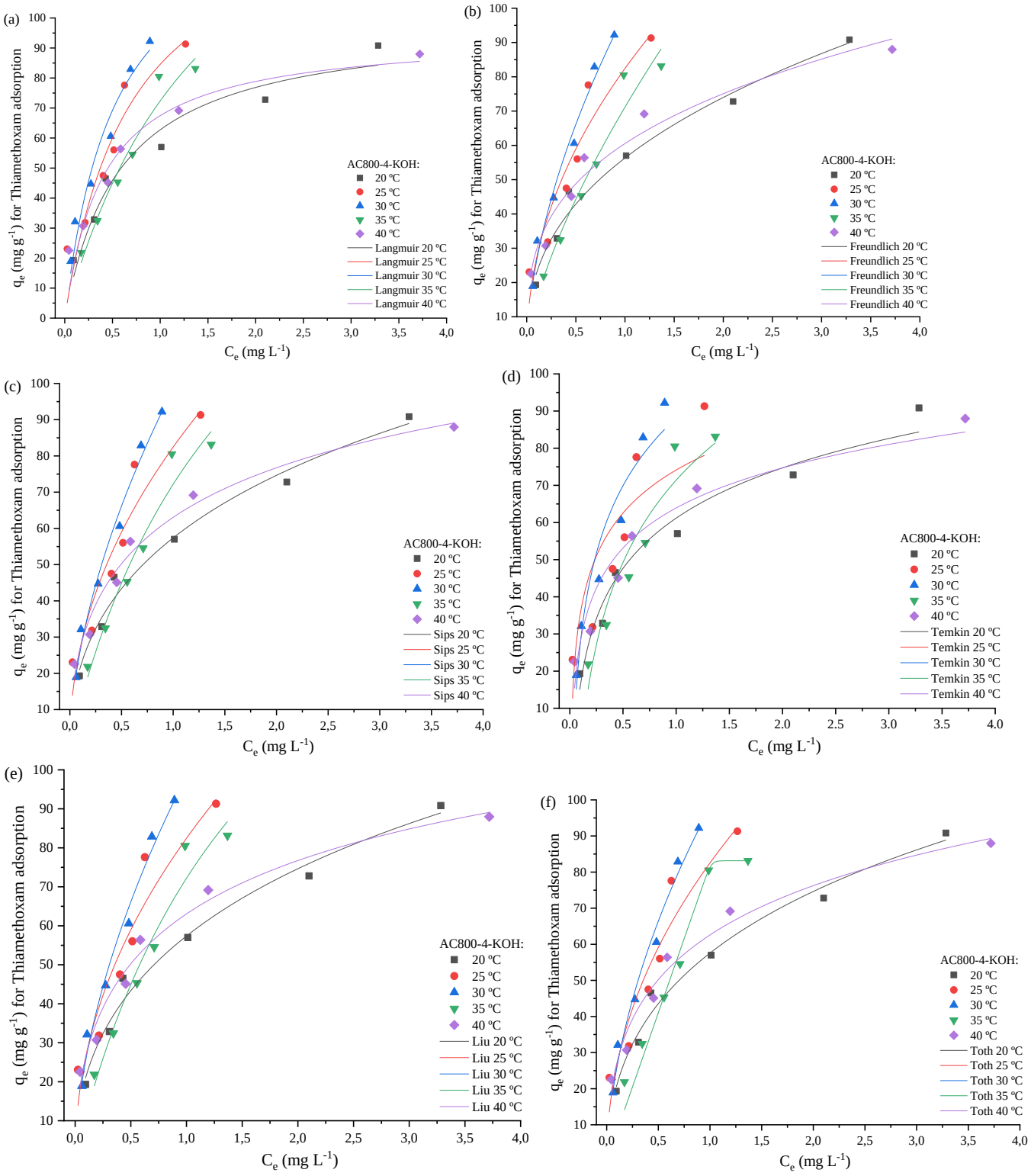

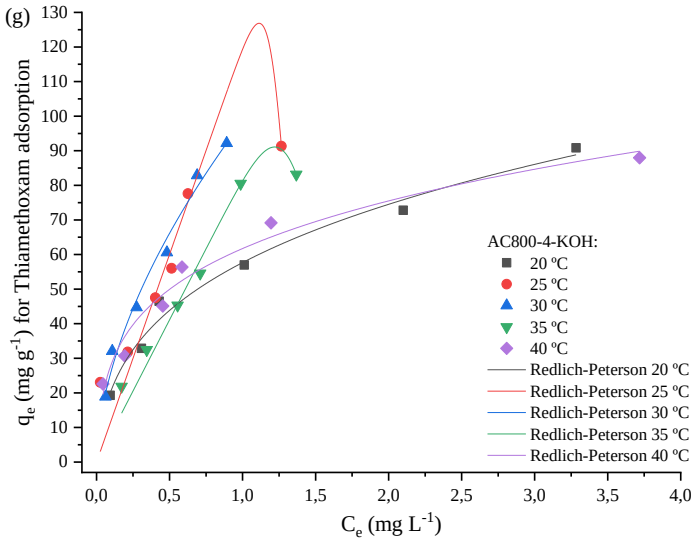
(g)
q_e (mg g^{-1}) for Thiamethoxam adsorption
C_e (mg L^{-1})
AC800-4-KOH:
20 °C
25 °C
30 °C
35 °C
40 °C
Redlich-Peterson 20 °C
Redlich-Peterson 25 °C
Redlich-Peterson 30 °C
Redlich-Peterson 35 °C
Redlich-Peterson 40 °C

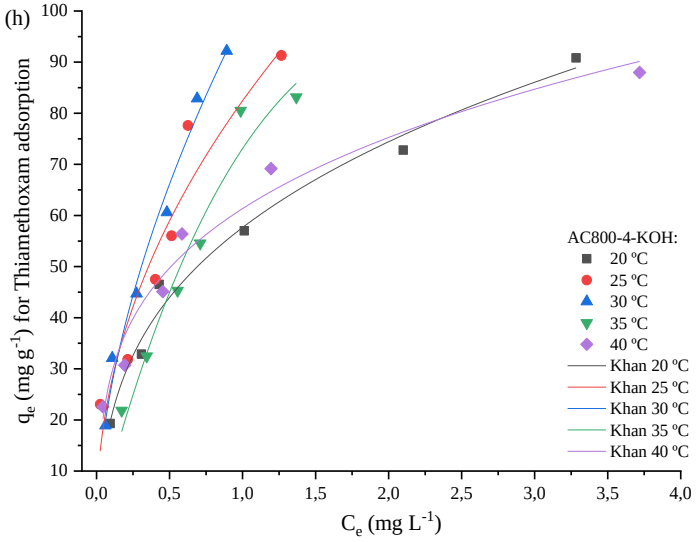
(h)
q_e (mg g^{-1}) for Thiamethoxam adsorption
C_e (mg L^{-1})
AC800-4-KOH:
20 °C
25 °C
30 °C
35 °C
40 °C
Khan 20 °C
Khan 25 °C
Khan 30 °C
Khan 35 °C
Khan 40 °C

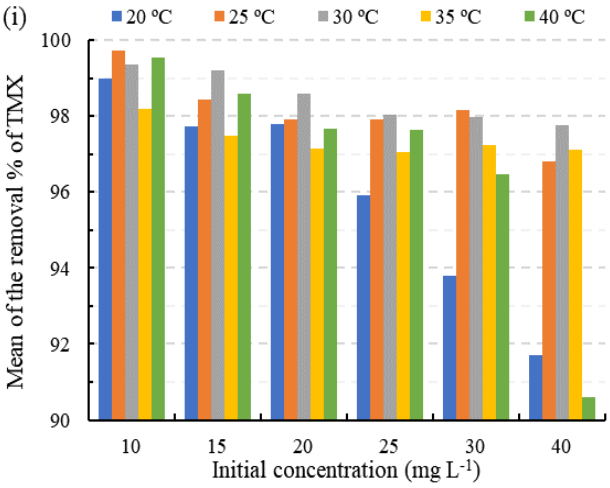
(i)
20 °C
25 °C
30 °C
35 °C
40 °C
Mean of the removal % of TMX
Initial concentration (mg L^{-1})

Figure S 2.2 - Thiamethoxam (TMX) adsorption isotherms for AC900-4-KOH at different temperatures (20, 25, 30, 35, and 40 °C) according to nonlinear models of Langmuir (a), Freundlich (b), Sips (c), Temkin (d), Liu (e), Toth (f), Redlich - Peterson (g) and Khan (h); Variation of Thiamethoxam removal by AC900-4-KOH as a function of different temperatures and initial concentration of insecticide (i). Experimental conditions: 0.01 g of adsorbent, pH 5.0, contact time of 40 min., 200 rpm. Variables: Temperature 20, 25, 30, 35 and 40 °C, and thiamethoxam concentration: 10, 15, 20, 25, 30 e 40 mg L^{-1}.

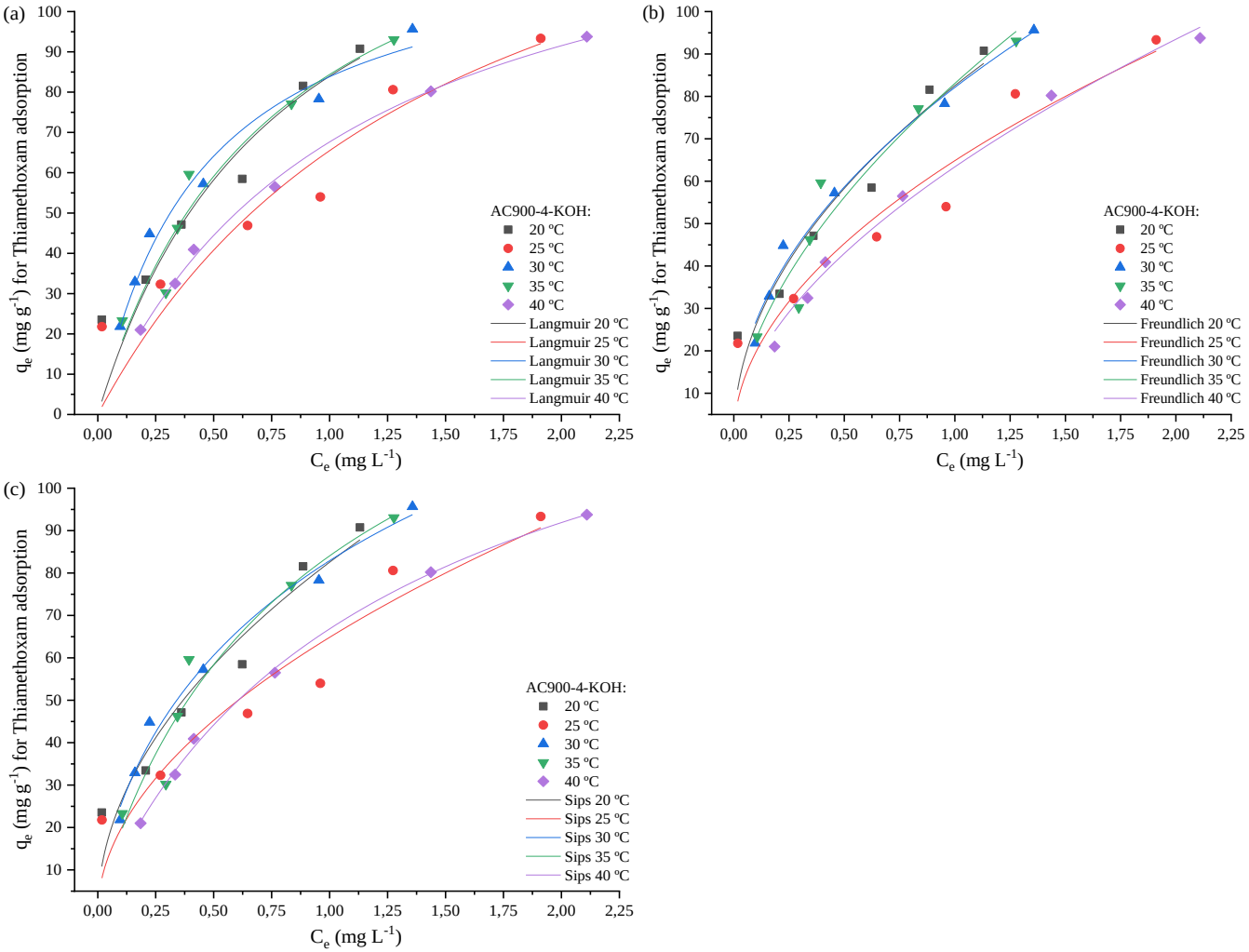

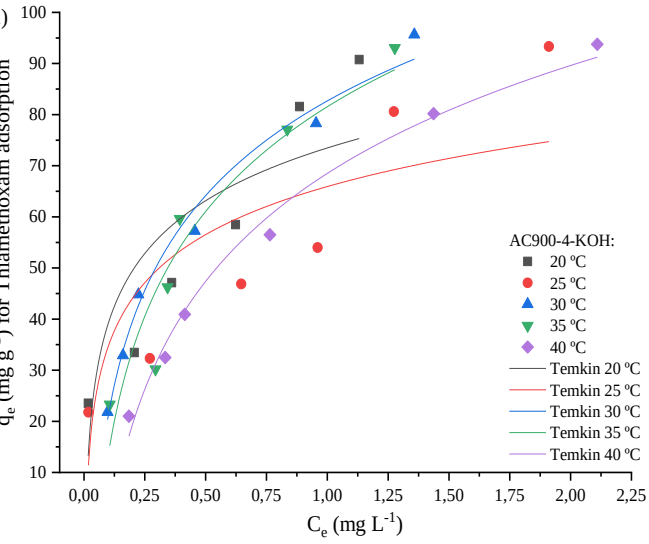
q_e (mg g^{-1}) for Thiamethoxam adsorption
C_e (mg L^{-1})
AC900-4-KOH:
20 ºC
25 ºC
30 ºC
35 ºC
40 ºC
Temkin 20 ºC
Temkin 25 ºC
Temkin 30 ºC
Temkin 35 ºC
Temkin 40 ºC

(e)

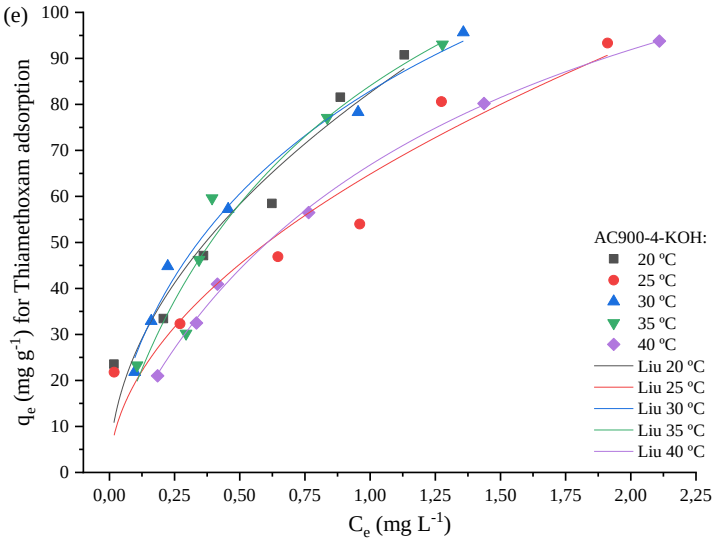
q_e (mg g^{-1}) for Thiamethoxam adsorption
C_e (mg L^{-1})
AC900-4-KOH:
20 ºC
25 ºC
30 ºC
35 ºC
40 ºC
Liu 20 ºC
Liu 25 ºC
Liu 30 ºC
Liu 35 ºC
Liu 40 ºC

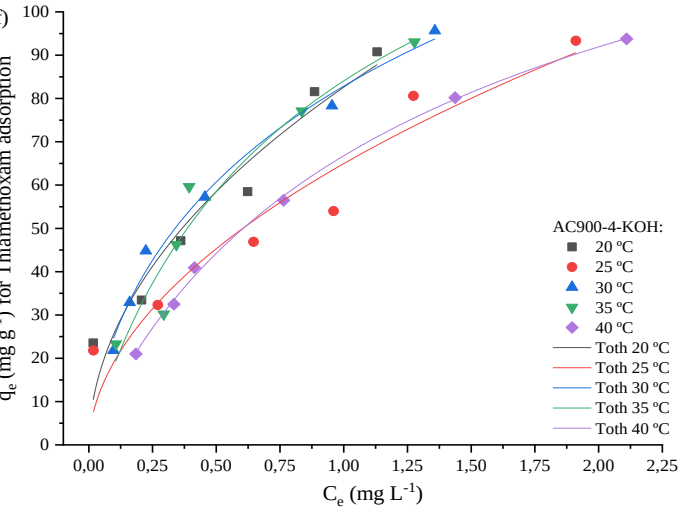
q_e (mg g^{-1}) for Thiamethoxam adsorption
C_e (mg L^{-1})
AC900-4-KOH:
20 ºC
25 ºC
30 ºC
35 ºC
40 ºC
Toth 20 ºC
Toth 25 ºC
Toth 30 ºC
Toth 35 ºC
Toth 40 ºC

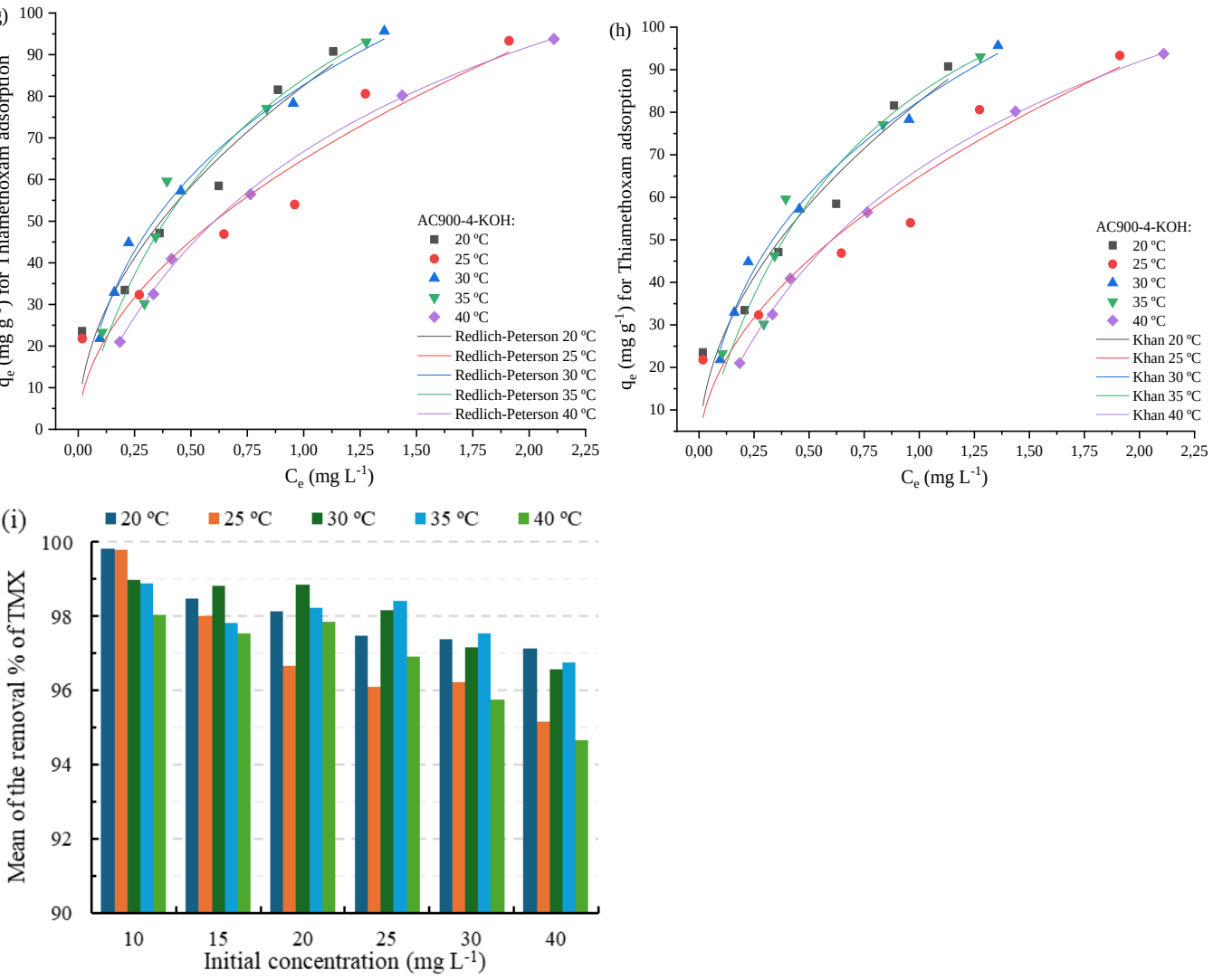

Figure S 2.3 - Thiamethoxam (TMX) adsorption isotherms for AC900-5-KOH at different temperatures (20, 25, 30, 35, and 40 °C) according to nonlinear models of Langmuir (a), Freundlich (b), Sips (c), Temkin (d), Liu (e), Toth (f), Redlich -Peterson (g) and Khan (h); Variation of Thiamethoxam removal by AC900-5-KOH as a function of different temperatures and initial concentration of insecticide (i). Experimental conditions: 0.01 g of adsorbent, pH 5.0, contact time of 40 min., 200 rpm. Variables: Temperature 20, 25, 30, 35 and 40 °C, and thiamethoxam concentration: 10, 15, 20, 25, 30 e 40 mg L $^{-1}$.

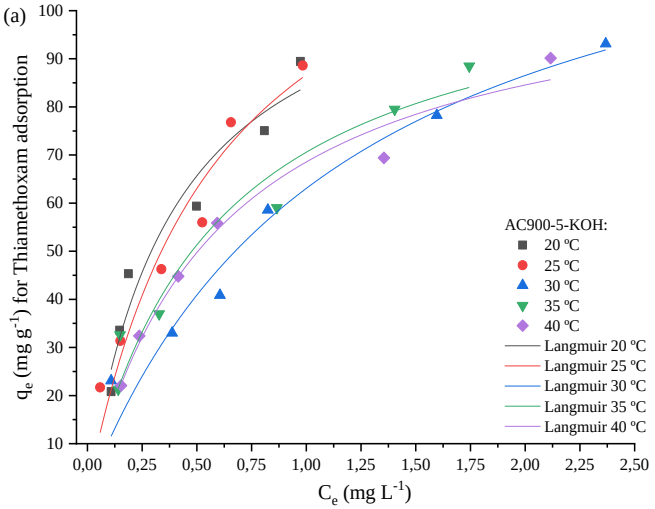
(a)
q_e (mg g^{-1}) for Thiamethoxam adsorption
C_e (mg L^{-1})
AC900-5-KOH:
20 ºC
25 ºC
30 ºC
35 ºC
40 ºC
Langmuir 20 ºC
Langmuir 25 ºC
Langmuir 30 ºC
Langmuir 35 ºC
Langmuir 40 ºC

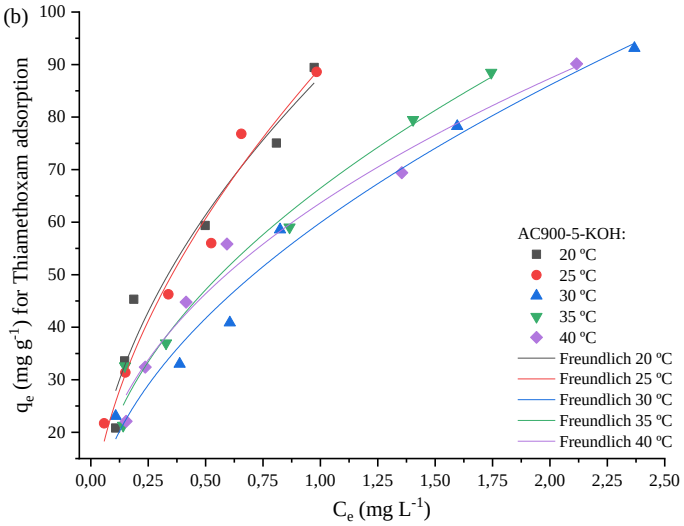
(b)
q_e (mg g^{-1}) for Thiamethoxam adsorption
C_e (mg L^{-1})
AC900-5-KOH:
20 ºC
25 ºC
30 ºC
35 ºC
40 ºC
Freundlich 20 ºC
Freundlich 25 ºC
Freundlich 30 ºC
Freundlich 35 ºC
Freundlich 40 ºC

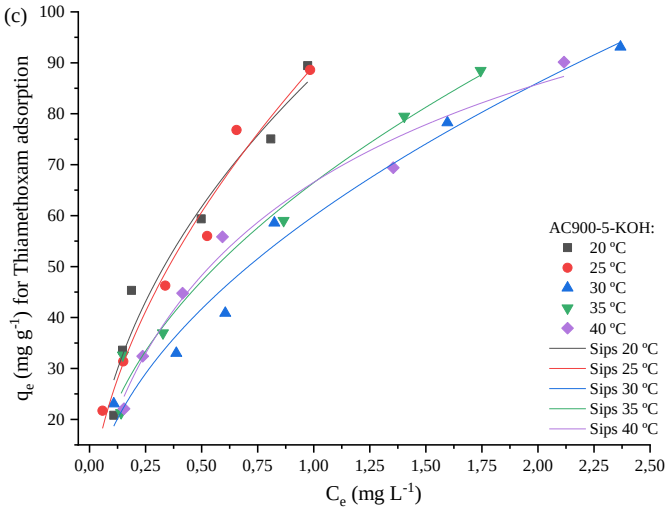
(c)
q_e (mg g^{-1}) for Thiamethoxam adsorption
C_e (mg L^{-1})
AC900-5-KOH:
20 ºC
25 ºC
30 ºC
35 ºC
40 ºC
Sips 20 ºC
Sips 25 ºC
Sips 30 ºC
Sips 35 ºC
Sips 40 ºC

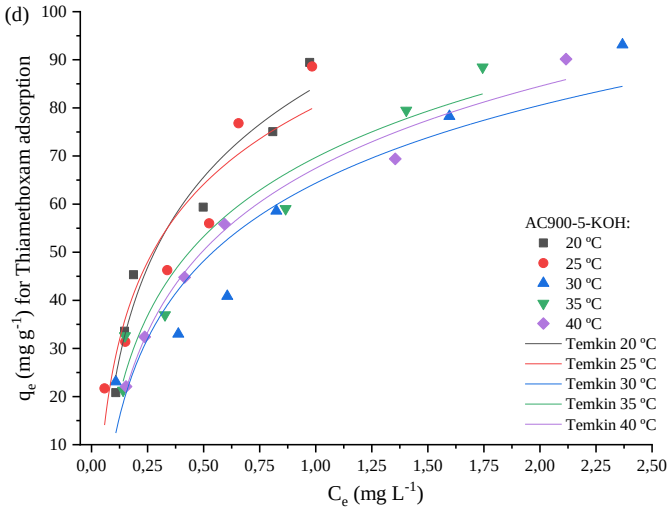
(d)
q_e (mg g^{-1}) for Thiamethoxam adsorption
C_e (mg L^{-1})
AC900-5-KOH:
20 °C
25 °C
30 °C
35 °C
40 °C
Temkin 20 °C
Temkin 25 °C
Temkin 30 °C
Temkin 35 °C
Temkin 40 °C

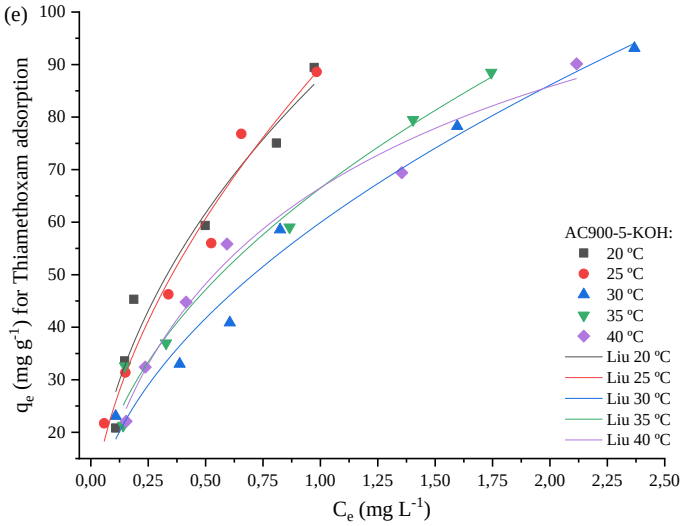
(e)
q_e (mg g^{-1}) for Thiamethoxam adsorption
C_e (mg L^{-1})
AC900-5-KOH:
20 °C
25 °C
30 °C
35 °C
40 °C
Liu 20 °C
Liu 25 °C
Liu 30 °C
Liu 35 °C
Liu 40 °C

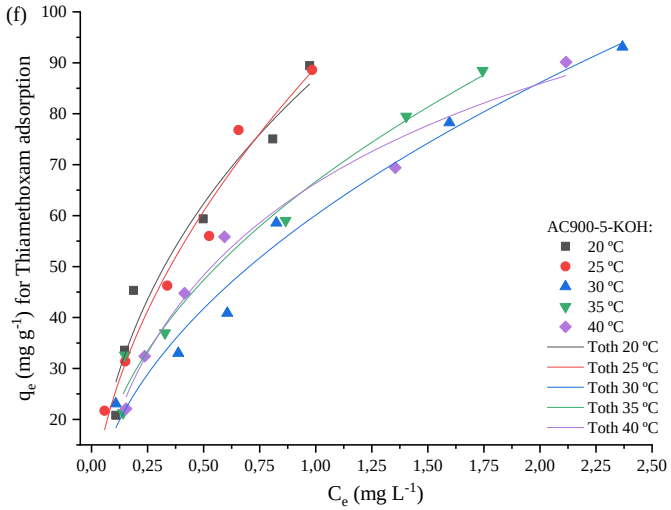
(f)
q_e (mg g^{-1}) for Thiamethoxam adsorption
C_e (mg L^{-1})
AC900-5-KOH:
20 °C
25 °C
30 °C
35 °C
40 °C
Toth 20 °C
Toth 25 °C
Toth 30 °C
Toth 35 °C
Toth 40 °C

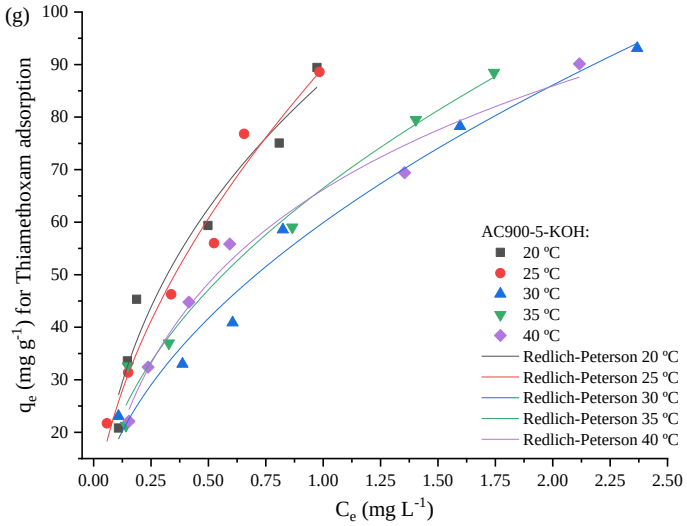
(g)
q_e (mg g^{-1}) for Thiamethoxam adsorption
C_e (mg L^{-1})
AC900-5-KOH:
20 °C
25 °C
30 °C
35 °C
40 °C
Redlich-Peterson 20 °C
Redlich-Peterson 25 °C
Redlich-Peterson 30 °C
Redlich-Peterson 35 °C
Redlich-Peterson 40 °C

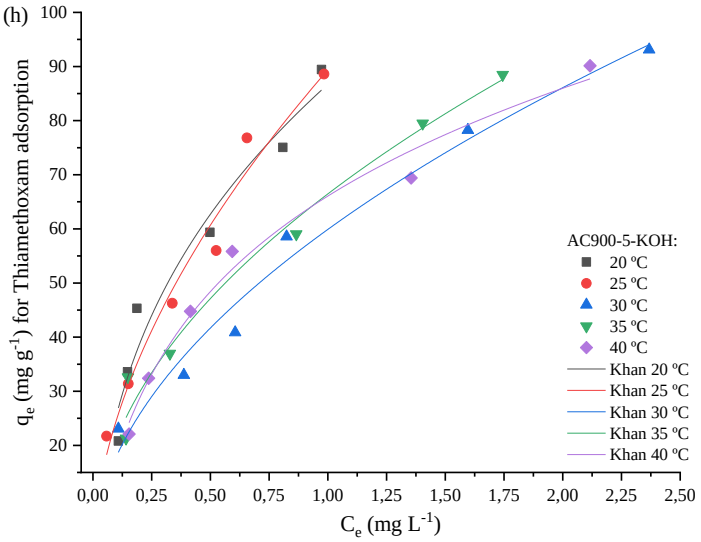
(h)
q_e (mg g^{-1}) for Thiamethoxam adsorption
C_e (mg L^{-1})
AC900-5-KOH:
20 °C
25 °C
30 °C
35 °C
40 °C
Khan 20 °C
Khan 25 °C
Khan 30 °C
Khan 35 °C
Khan 40 °C

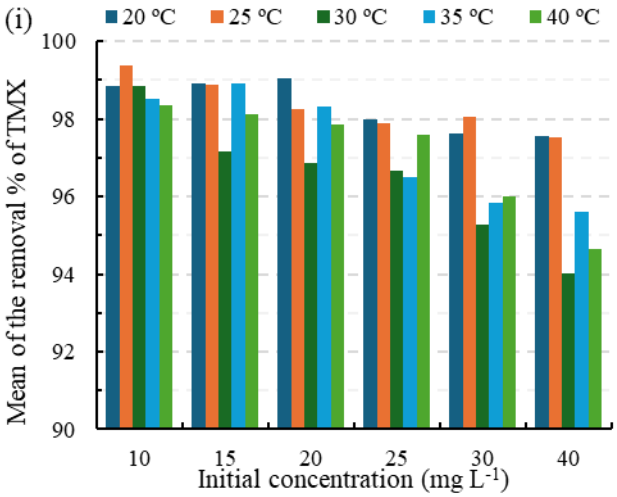
(i)
20 °C
25 °C
30 °C
35 °C
40 °C
Mean of the removal % of TMX
Initial concentration (mg L^{-1})